Journal of Applied Electrochemistry **31**: 155–164, 2001.

Cathodic refining in molten salts: Removal of oxygen, sulfur and selenium from static and flowing molten copper

G.Z. CHEN and D.J. FRAY*
Department of Materials Sciences and Metallurgy, University of Cambridge, Pembroke Street, Cambridge, UK CB2 3QZ
*(*author for correspondence, e-mail: djf25@hermes.cam.ac.uk)*

Received 5 June 2000; accepted in revised form 22 August 2000

Key words: cathodic refining, copper, molten salts, recessed channel electrode

Abstract

The removal of nonmetallic impurities, including oxygen, sulfur and selenium, from molten copper (cathode) was achieved by constant voltage electrolysis in molten $BaCl_2$ and $CaCl_2$ alone, or the eutectic mixture of the two at temperatures slightly higher than the melting point of copper. At the applied voltages (2.1 $\sim$ 2.9 V), the cathodic refining occurred without provoking the decomposition of the chloride salts, demonstrating the cathodic ionization of impurities to be responsible. Further evidence supporting this mechanism came from SEM, EDX and preliminary voltammetric studies. To increase the mass transfer of the impurities in the molten copper during the refining process, a novel recessed channel electrode (RCE) was used. The results have demonstrated the feasibility and efficiency of using this technology in terms of space, time and yield of product, offering considerable advantages over a simple electrorefining cell.

1. Introduction

Metals like copper and iron are usually refined pyrometallurgically by using oxygen or air as a refining agent to remove the more reactive elements. The elimination of the final amounts of residual oxygen is achieved by adding deoxidants to the molten metal. For example, aluminium, calcium, silicon or manganese are used as the deoxidant in the case of steel [1] and phosphorus in the case of copper [2]. Usually, the deoxidants form inclusions with the oxygen. These inclusion compounds can either float to the surface region of the molten metal or become entrapped in the metal on solidification [1]. Additionally, as is the case with copper, any excess phosphorus over that required to remove the oxygen remains in the copper to the detriment of the properties of the metal [2]. With the advent of the concept of 'clean metals' it is paramount to consider alternative ways of removing the final quantities of impurities from molten metals without introducing reagents and/or creating inclusions. This challenge makes electrochemical techniques the most suitable choice as the role of a deoxidant can be ideally replaced by electrons which can be provided to the metals via inert electrodes and/or current collectors.

Electrorefining of metals is usually considered in terms of making the metal phase the anode and ionizing the most reactive elements into the electrolyte. The ionized elements are then transported to and plated out at the cathode. This principle can been seen in the cases of refining copper in aqueous electrolyte and aluminium in molten salt electrolyte [2, 3]. However, there are considerable advantages if the impurities can be ionized, leaving the pure metal. This can occur if the metal is made the cathode in a molten salt containing ions of a very electropositive element such as barium [4] and calcium. If we consider the cathodic removal of nonmetallic impurities such as oxygen, sulfur and selenium from metals in molten $CaCl_2$, there are two types of possible cathodic reaction:

(i) deposition of calcium metal

$$Ca^{2+} + 2e = Ca \quad E_{vs\,Ca^{2+}|Ca} = 0\,V$$

(ii) cathodic ionization of the impurities

$$\tfrac{1}{2}O_2(g)(\text{or } O_{m|e}) + 2e^- = O^{2-} \quad E_{vs\,Ca^{2+}|Ca} = 2.60\,V$$
$$\tfrac{1}{2}S_2(g)(\text{or } S_{m|e}) + 2e^- = S^{2-} \quad E_{vs\,Ca^{2+}|Ca} = 2.14\,V$$
$$\tfrac{1}{2}Se_2(g)(\text{or } Se_{m|e}) + 2e^- = Se^{2-} \quad E_{vs\,Ca^{2+}|Ca} = 1.63\,V$$

where $O_{m|e}$, $S_{m|e}$ and $S_{m|e}$ stand for the respective impurities at the metal electrolyte interface. The ionization potentials of the impurities are calculated from the formation Gibbs free energy of CaO, CaS and CaSe, respectively, at 1000 °C [5, 6]. In the calculation, it is assumed that CaO, CaS and CaSe dissociate completely

in molten $CaCl_2$ (should the dissociation be incomplete, the ionization potentials would be more positive). It can be seen that the cathodic ionization of the three impurities in the presence of Ca^{2+} is much more favoured over the calcium deposition. This forms the basis of this research work.

It is acknowledged that the calculated potentials are for the impurities at unit activity. However, there are such large differences in electrode potentials that the cathodic removal of these impurities could still be the preferred reactions even at the ppm level. This expectation is based on the Nernst equation according to which, for oxygen at 1000 °C, the negative (cathodic) potential shift of 2.60 V is equivalent to a decrease of more than 42 orders of magnitude in the equilibrium partial pressure of oxygen. Similarly for sulfur and selenium, their partial pressures can be 34 and 26 orders of magnitudes lower, respectively, when the potential is shifted to that of calcium deposition.

In practice, if the ionized impurities were not soluble in the electrolyte, they could accumulate on the surface of the metal to be refined, and the ionization would cease shortly after applying the cathodic potential. Therefore, it is crucial that the molten salt used must have a sufficiently high solubility for the ionized impurities or their compounds formed with the molten salt or one of its components. It is known that both $BaCl_2$ and $CaCl_2$ can accommodate a reasonably large quantity of oxygen in the form of either O^{2-} or BaO or CaO (the solubility of BaO in $BaCl_2$ is about 45 mol% and CaO in $CaCl_2$ about 20 mol% at 1160 °C [7]). This allows the ionized oxygen to dissolve in the melt, diffuse to the anode where it is discharged as the oxygen gas which may further react with the anode, if made from carbon, to produce carbon oxides, CO_2 and/or CO. Similar information on sulfur and selenium is rare, if not unavailable, in the literature, but we expect that the two elements are not too different from oxygen.

Another practical challenge is that when applying the principle of cathodic ionization to refine a static metal pool, especially at low impurity concentrations, the rates of removal are expected to be controlled by the diffusion of the impurity species to the metal|electrolyte interface. As mentioned by Ward and Hoar [4], this can be an intractable problem when the metal pool is deep. Furthermore, the refining of large pools of metal is likely to occupy a large area of floor space making the process untenable [4]. These problems can be overcome by using a novel recessed channel electrode (RCE) as shown schematically in Figure 1. In the RCE, the molten metal flows down channels in the electrode surface creating a well mixed phase with small diffusion distances [9, 10]. In addition, because the anode to cathode distance, determined by the thickness of the diaphragm, is very narrow, the *IR* drop of the electrolyte between electrodes is minimal. This can be compared with conventional molten salt electrorefining cells where stagnant pools of metal are separated by a substantial thickness of electrolyte.

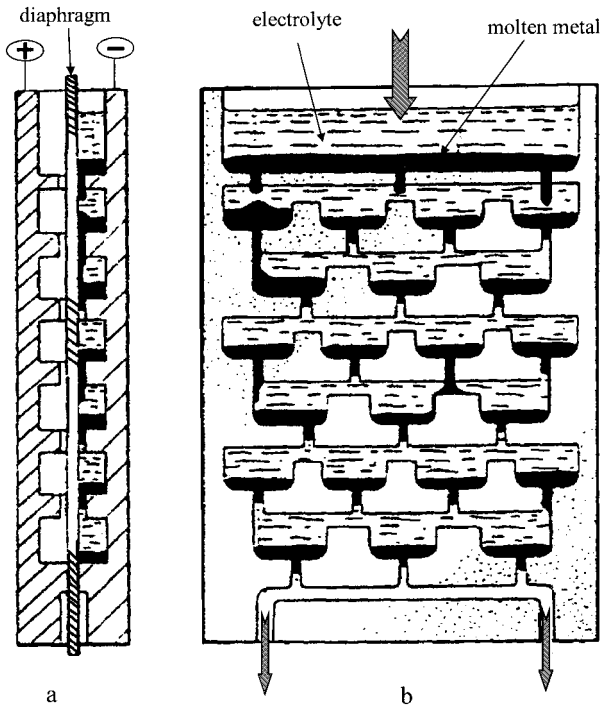

Fig. 1. Schematic diagrams of (a) recessed channel electrode assembly and (b) details of the recessed channels in the electrode surface.

2. Experimental details

2.1. *Equipment and apparatus*

A vertical 1600 °C furnace (Lenton), equipped with a programmable controller and a sealable tube reactor, was used for heating purposes. The tube reactor was made from Inconel with the dimensions being 110 mm internal diameter, 650 mm length and 5 mm wall thickness. It had also a water cooled top jacket and an O-ring sealed lid assembly containing a number of holes for electrode insertion and inspection. The inspection holes (windows) were sealed by glass and rubber rings. For electrolysis, the current or voltage was controlled by a Farnell LS30-10 Autoranging power supply. Electroanalytical measurements were performed on an EG&G Princeton Applied Research potentiostat/galvanostat model 273A, together with the m270 software. Figure 2(a) shows schematically the electrolytic cell set-up.

2.2. *Materials and chemicals*

Copper containing oxygen up to 5500 ppm and various other impurities was obtained from IMI Refiners. High density graphite material used for fabricating electrolytic cells was purchased from Graphite Technologies. A specially long graphite rod (9.5 mm dia. × 600 mm length) used as the anode was bought from Multi-Lab. Alumina crucibles and porous diaphragms were made in-house. Graphi-Bond, for fixing the diaphragm to the recessed channel cell, was purchased from Component & Produces. Pure argon, (> 99.99%) from Air Products, was used to purge air from the reactor. All other

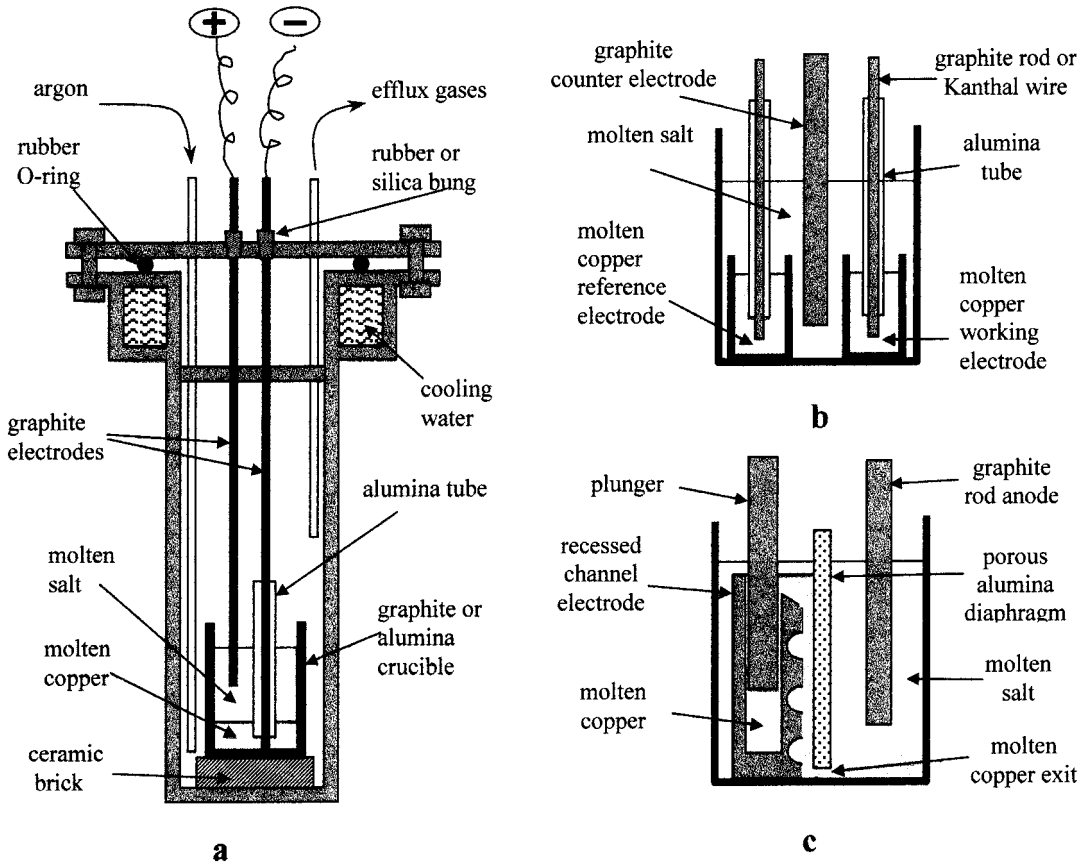

Fig. 2. Schematic diagrams of (a, left) reactor and crucible cell for electrolysis of static molten copper, (b, upper right) electrochemical cell for voltammetry of molten copper, and (c, bottom right) recessed channel electrode and cell assembly used for electrolysis of flowing molten copper.

chemicals, including $CaCl_2$ (anhydrous and dihydrate), $BaCl_2$ (dihydrate) and copper shot of the ACS or a higher grade were purchased from Aldrich.

2.3. *Environmental control in the tube reactor*

A dry argon environment with a small positive pressure in the reactor was maintained during all reactions by an argon flow which was introduced into the reactor via a pair of molecular sieves and self-indicating silica gel columns at the rate of about 150 cm^3 min^{-1}. The exiting gases, expected to contain the gas products of anodic reactions, were guided via another pair of molecular sieves and silica gel columns into a bottle of sulfuric acid (>98%) before escaping to the atmosphere. The after-reactor gas-columns and sulfuric acid were used for trapping and therefore preventing the backward diffusion of moisture. The colour of the silica gel was also a convenient indication of the dryness of existing gases. In addition, the heavy sulfuric acid helped to maintain a positive argon pressure in the reaction system. This was achieved by adjusting the depth of the open end of the gas-outlet tube underneath the surface of the acid to about 100 mm at which the corresponding positive pressure would be 14.2 mm Hg higher than the atmosphere.

2.4. *Analysis of the effluent gases of electrolysis*

The effluent gases of electrolysis were sampled at different times of the experiment. Sampling was carried out using 50 ml syringes at the gas-outlet tube before the drying columns. The syringes were flushed with the effluent gases at least three times prior to sampling. The collected samples were immediately subjected to a Chrompack CP9001 gas chromatograph (GC). The gas column of this GC was not capable of separating oxygen and argon. Therefore oxygen contained in the effluent gases was analysed by applying deoxygenated dry nitrogen as the purging gas during electrolysis.

2.5. *Sample characterization*

Optical microscopy was used for routine inspection of samples. Detailed microscopic information was obtained from the Jeol5800LV scanning electron microscope which was also capable of performing EDX (energy dispersive X-ray analysis). While calcium and barium in the electrolysed samples were analysed by EDX in this department, the fusion elemental analyses of oxygen, sulfur and selenium were carried out by IMI Refiners.

2.6. *Electrochemistry*

All electrochemical experiments were conducted in a thermally dried chloride melt that was contained in a cylindrical crucible made from either alumina or graphite. Ward and Hoar [4] claimed that, in addition to electrochemistry, a direct reaction between the oxygen in the molten copper and the graphite crucible (cathodic current collector) was also responsible for the removal of oxygen from molten copper. The use of alumina crucibles in this work was therefore to demonstrate whether or not the deoxidation of molten copper could be achieved completely electrochemically.

The electrolysis of a static molten copper pool in a molten salt, i.e. $CaCl_2$ or $BaCl_2$, was performed at 1160 °C in a manner of two-electrode and constant voltage (Figure 2(a)). A graphite rod was used as the anode and the copper sample as the cathode. The graphite anode had a surface area of about 10 cm^2 (9.5 mm diameter and 30 $\sim$ 35 mm depth). The surface area of the molten copper cathode was confined by the internal diameter of the crucible. The dimensions of the crucibles were (a) 55 mm internal diameter, 100 mm depth and 3 mm wall thickness for the alumina crucible and (b) 30 mm internal diameter, 85 mm depth and 10 mm wall thickness for the graphite crucible. The copper sample was placed in the crucible which was subsequently filled to the rim with the dry salt powder and heated to the working temperatures under argon.

The molten copper cathode was linked to the power supply via a current collector made from a Kanthal wire or graphite rod. In the graphite crucible, the cathodic current was collected by a Kanthal wire basket tightly fitted to the external wall of the graphite crucible. This not only simplified the experimental procedure but also allowed the use of smaller crucibles in which only the anode is needed to be placed in the molten salt.

Three-electrode voltammetry was applied to study the electrochemical nature of the impure molten copper in molten $CaCl_2$ at 1160 °C. In these cases, the molten copper was used as the working electrode, contained in a small alumina crucible which was placed at the bottom of a large alumina crucible. The surface area of the molten copper was about 1 cm^2. A second molten copper electrode was used as a pseudo-reference electrode. The calcium deposition reaction, $Ca^{2+} + 2\,e^- = Ca$, was used as an internal reference. A graphite rod functioned as the counter electrode. Figure 2(b) shows schematically the voltammetric cell configuration. We would like point out that recording the voltammograms of molten copper in molten salt was highly challenging for a number of reasons. One of these is due to the large surface area of the molten metal electrode and the high working temperature, resulting in a large current flow which leads to a high *IR* distortion on the shape of the obtained CVs. A positive feedback *IR* compensation was applied to reduce the distortion. However, it was found that the *IR* level changed with time in an irregular manner, and therefore causing some inconsistency.

The electrolysis of flowing molten copper was realized via the recessed channel electrode (RCE), see Figures 1 and 2(c). A rigid porous alumina tile was attached to the graphite RCE by Graphi-Bond as the diaphragm which also confined the flow of molten copper to the recessed channels of the RCE. A grooved pathway was incorporated between the reservoir and the recessed channels. This ensured that the metal exuded out of the reservoir went through the recessed channels and did not spill over into the molten salt. An experiment without the sloped pathway showed clearly that the molten copper did not enter the channels. Finally, because the impurities took part in the cathodic reactions and the molten metal remained in the recessed channels until it travelled down to the exit, it was found to be much more convenient to just use the cathodic part of the RCE. An independent graphite rod functioned as the anode in this work, although the anodic part of the RCE (Figure 1) should be applied in practical applications.

With the hope of improving the flowability of the molten copper in the pathway and channels, the RCE electrolysis was performed at 1250 °C, higher than that used in the static cases (1160 °C). In addition, instead of a single salt melt, the eutectic mixture of $BaCl_2$ and $CaCl_2$ (m.p. 600 °C [8]) was used in the RCE experiment. It was thought the observed high residual current in $CaCl_2$ (discussed in the main text) could be reduced by the addition of $BaCl_2$.

During the RCE experiment, the copper sample was first stored in the reservoir and later, after melting, transferred to the channels by a manually operated plunger in a step-by-step manner. At each step, the insertion was about 2.5 mm with the time between neighbouring steps being 2 $\sim$ 5 min. Upon applying the voltage, the current flow followed a similar pattern to the static case, but was not very much affected by the insertion of the plunger. This is not surprising taking into account the large background current resulting from the large surface area of the whole RCE in touch with the melt.

The Graphi-Bond used to bond the diaphragm to the RCE is very stable in the molten salts used. After electrolysis, the diaphragm could be easily removed from the RCE by disintegrating the Graphi-Bond in water. This property of Graphi-Bond is very useful for the reuse of all or part of the bonded materials in laboratory practice.

3. Results and discussion

3.1. *Microscopic features of oxygenated copper*

Figure 3 shows two microphotographs taken from oxygenated copper samples used in this work. It is worthy of noting that although not very accurate for quantitative oxygen analysis, optical microscopy is effective for identifying the presence of oxygen in copper samples. The lower limit can be as little as 200 ppm [11].

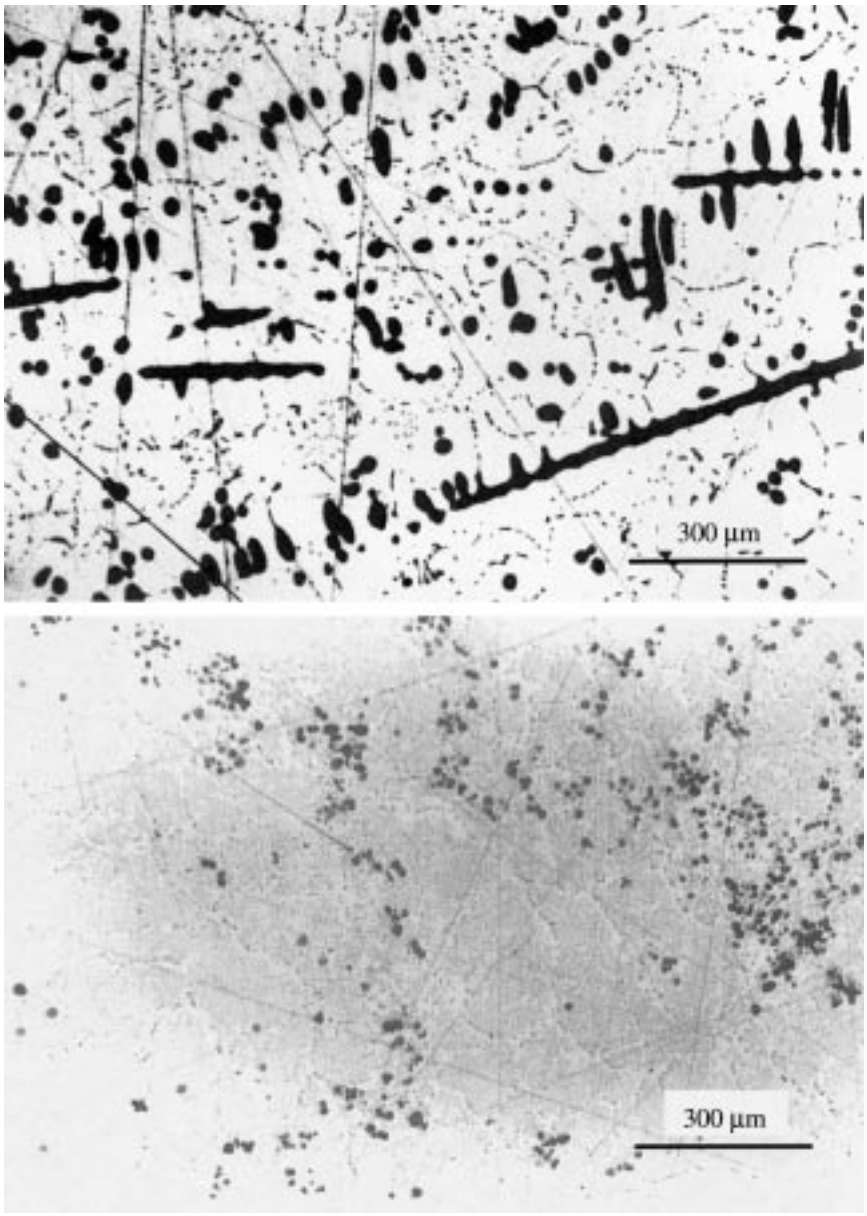

Fig. 3. Optical microphotographs of (upper) an oxygenated copper sample prepared by heating copper (50.0 g, ~1000 ppm oxygen) with CuO (1.0 g) and molten NaCl (24.0 g) in air slowly to 1300 °C for about 40 min, and (lower) the copper sample obtained from IMI Refiners Ltd containing 5500 ppm oxygen.

3.2. *Molten salts*

It was found that the rate of temperature increase was crucial in drying the salts with the slower rate resulting in less retained water in the melt. For practical reasons, 0.2 °C min^{-1} was applied in this work. It needs to point out that a trace amount of moisture was always found in thermally dried melts, as indicated by preelectrolysis at 2.5 ~ 2.7 V. Nevertheless, for refining copper, this trace amount of water did not show significant effect on the result.

Vapourization of molten $CaCl_2$ at elevated temperatures (> 1000 °C) was observed. However, at the same temperatures, molten $BaCl_2$ and the eutectic mixture of $BaCl_2$ and $CaCl_2$ were found to be much more stable.

3.3. *Current variation with time during electrolysis*

Upon applying the voltage (2.1 ~ 2.7 V), the responding current for both $CaCl_2$ and $BaCl_2$ fluctuated irregularly in the beginning and decayed continuously with time. Table 1 lists the current measured during the experiments. The fluctuation gradually disappeared after 15 ~ 30 min of the electrolysis. Current fluctuation is often an indication of the formation and escape of gas bubbles on one or both of the two electrodes. Indeed, significant bubbling around the anode was observed in the beginning of electrolysis. There are two possible origins for the gas evolution. The first possibility may be related with the residual moisture contained in the melt which was only thermally dried in air, although preelectrolysis or dry HCl/Cl_2 gas bubbling could further

Table 1. Current variation during the electrolysis of the copper sample from IMI Refiners Ltd at 1160 °C

$BaCl_2$	Time/min	1	3	23	53	95	120
2.6 V	Current/A	2.80 ± 0.5	2.45 ± 0.3	0.47	0.26	0.13	0.14
$CaCl_2$	Time/min	1	3	18	50	80	133
2.6 V	Current/A	2.5 ± 0.5	2.70 ± 0.3	2.50	0.97	1.03	1.35
$BaCl_2$	Time/min	2	13	22	41	85	120
2.1 V	Current/A	2.0 ± 0.5	1.6 ± 0.3	0.73	0.16	0.05	0.07
$CaCl_2$	Time/min	1	5	15	46	108	122
2.1 V	Current/A	2.95 ± 0.5	2.93 ± 0.5	2.50	1.10	0.44	0.41

improve the dryness of the melt. The second origin, that is more likely the dominant factor, is the discharge of the ionized impurities, particularly oxygen. The gas evolution at the anode would gradually decrease as the supply of ionized impurities from the copper declines with the time of electrolysis. Our GC analysis showed that the effluent gases were a mixture of O_2 and CO in a roughly volume ratio up to 1:1. The detection of oxygen is interesting but not surprising as previous studies have shown that the reaction between oxygen and carbon at moderate temperatures is strongly affected by kinetic factors including material texture/structure, presence of inhibitors such as silicon, boron and phosphorus (common impurities in commercial graphite), and types of molten salts [12–15]. Chlorine was never detected in the effluent gases. Other gases, particularly the targeted S_2 and Se_2, were neither detected and the condensed forms of the two elements or their compounds were not visible in the solidified salt, apparently due to their very low initial concentrations in the copper samples.

In Figure 4 are shown the current–time relations recorded during the electrolysis in both $BaCl_2$ and $CaCl_2$ melts. The continuous decaying of the current at a fixed voltage confirms that impurities are being removed and alkaline earth metals are not being deposited, otherwise the current would have remained constant with time.

Interestingly, it can be seen in Figure 4 that the current flow in $CaCl_2$ is much greater than in $BaCl_2$. This contradicts with the fact that $BaCl_2$ can accommodate more ionized oxygen than $CaCl_2$. In fact, the impurity levels detected in samples electrolysed in $BaCl_2$ were lower than that in $CaCl_2$ (Table 2). Therefore, it is difficult to attribute the observed higher current in $CaCl_2$ to a higher rate for impurity ionization. A closer inspection of Figure 4 revealed that the differences in the initial and final current between the two curves are roughly 0.5 A, implying a higher residual current in $CaCl_2$.

To further understand this phenomenon, current–voltage relations were recorded in the two melts before and after electrolysis. Typical examples are presented in Figure 5. It can be seen that the residual current in $CaCl_2$ is significantly higher than in $BaCl_2$ over a wide range of voltages. Similar results were obtained when using a graphite rod or a Kanthal wire as the cathode. Since the two salts used had similar purity levels and the two-hour electrolysis should have removed moisture from the melt, it is unlikely that the higher residual

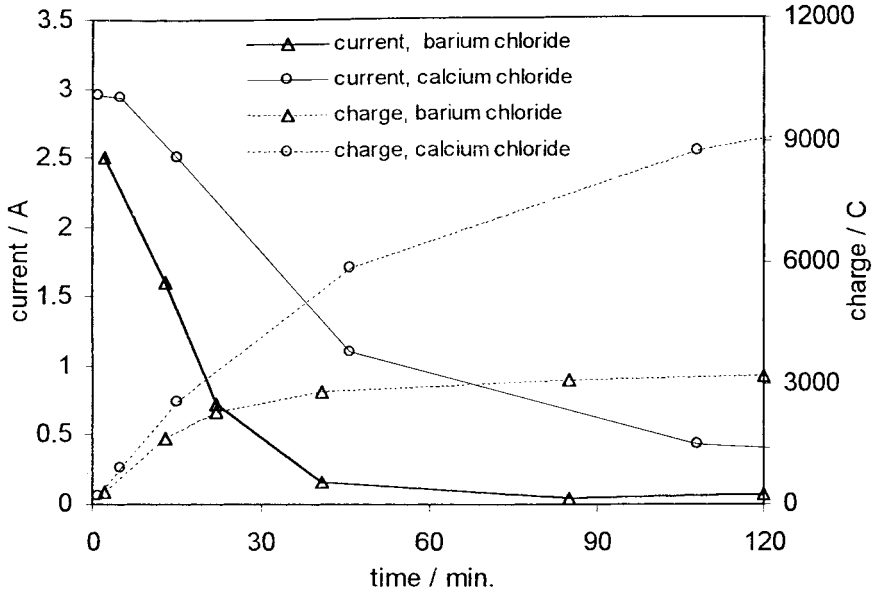

Fig. 4. Current–time and charge–time curves recorded during electrolysis of copper sample from IMI Refiners Ltd in molten $CaCl_2$ (○) and $BaCl_2$ (△) at 1160 °C. Applied voltage 2.1 V. Sample and molten salt contained in an alumina crucible. Sample connected to power supply via a Kanthal wire (o.d. 1.5 mm) protected in an alumina sheath. Graphite rod used as anode.

Table 2. Elemental analysis of the copper sample from IMI Refiner Ltd before and after electrolysis at 1160 °C for 2.0 h

	As-received	Electrolysed at 2.6 V in $BaCl_2$	Electrolysed at 2.6 V in $CaCl_2$	Electrolysed at 2.1 V in $BaCl_2$	Electrolysed at 2.1 V in $CaCl_2$
Oxygen/ppm	5500	30	100	50	100
Sulfur/ppm	10	Undetectable	Undetectable	Undetectable	Undetectable
Selenium/ppm	25	Undetectable	Undetectable	Undetectable	Undetectable

current in molten $CaCl_2$ was due to the redox processes of impurities. On the other hand, the residual current in molten $CaCl_2$ increased almost linearly with the voltage (Figure 5(b)), suggesting that $CaCl_2$ may have a higher electronic conductivity than $BaCl_2$ [16].

In addition, it can be seen in Figure 4 that, upon subtracting the residual current, the middle portion of the $CaCl_2$ curve is still higher than that of the $BaCl_2$ curve. While further work is needed for a full explanation, the following reactions are worth mentioning [5, 6].

$$Cu_2O + CaCl_2 = CaO + 2\,CuCl,$$
$$\Delta G^\circ(1160\ ^\circ C) = -38.780\,kJ$$
$$Cu_2O + BaCl_2 = BaO + 2\,CuCl,$$
$$\Delta G^\circ(1160\ ^\circ C) = 80.046\,kJ$$

When these reactions occur, a proportion of the current would be needed to recover the copper from the melt. Because copper ions can exist in two valent states (i.e., Cu^+ and Cu^{2+}), the anodic oxidation of Cu^+ to Cu^{2+} is inevitable. A worse scenario is the redox cycling of the Cu^+/Cu^{2+} couple between the cathode and anode, contributing to a larger current flow. Apparently, the opposite signs of the changes in Gibbs free energy for the two melts indicate that the redox cycling would be more serious in molten $CaCl_2$ in which the equilibrium concentration of Cu^+ ions would be about two orders of magnitude more than that in molten $BaCl_2$.

In accordance with this assumption, weight loss was commonplace in electrolysed samples. For example, after the electrolysis at 2.1 V, the weight loss was 1.3% in $CaCl_2$ and 1.1% in $BaCl_2$, both are greater than that expected from the total amount of impurities (less than 0.6%). However, the difference between the two weight losses is not as great as expected from the Gibbs free energy changes. This can be explained by that the electrolysis has recovered most of the copper from the melts. It was also noticed that the weight loss was less than 1% when the applied voltage was 2.6 V at which more copper could be recovered from the melt.

3.4. *Cyclic voltammetry*

To further clarify the suspected dissolution of Cu_2O into the melt, cyclic voltammetry of the molten copper sample was performed in $CaCl_2$. Figure 6 shows the cathodic branch of a CV of molten copper in $CaCl_2$. In this experiment, the anodic branch was not recorded because when the potential scan reached at the reversing potential, the current exceeded the limit of the potentiostat. Before the potential scan, the molten copper electrode was held at the rest potential, which was 0 with respect to the molten copper pseudo-reference electrode, until the current dropped to zero. It can be seen that two reduction processes are exhibited on the curve. The steady and continuously increasing current at the negative end of the potentials is obviously due to the deposition of calcium. The reduction current wave

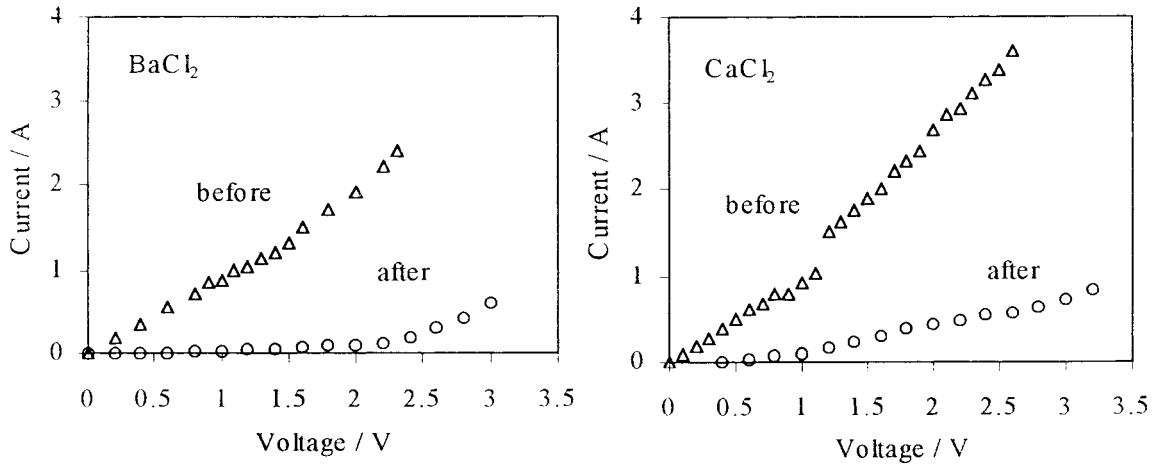

Fig. 5. I/V curves of the copper sample (same as that in Figure 4) recorded before (△) and after (○) electrolysis (2.0 h and 2.1 V) in molten $BaCl_2$ (left) and $CaCl_2$ (right) at 1160 °C. Graphite rod used as anode.

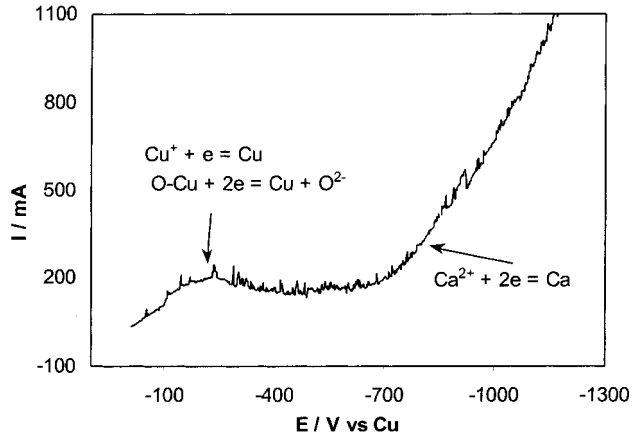

Fig. 6. Cathodic branch of a CV recorded in molten $CaCl_2$ from same oxygenated copper sample as in Figure 4. Surface area of working electrode ~1 cm^2; temperature 1160 °C; scan rate 50 mV s^{-1}.

centred at about −0.2 V is likely due to the redeposition of copper ions from the molten salt. However, it should be pointed out that this reduction wave is only about 0.5 V more positive than that of calcium deposition, far smaller than the calculated value of 1.98 V for the difference between the decomposition voltages of CuCl and $CaCl_2$ at our working temperature [5, 6]. This is surprising even taking into account the fact that calcium metal is completely miscible with molten copper, resulting in a positive shift of the calcium deposition potential.

An alternative explanation is that the reduction wave at −0.2 V might have resulted from the ionization of oxygen. According to the phase diagram [17], the oxygen contained in our copper sample should be fully dissolved in molten copper. Therefore, the reaction between Cu_2O and $CaCl_2$ may not proceed to the completion, leaving a sufficient amount of oxygen in the molten copper. Because the activity of the dissolved oxygen is much lower than that in Cu_2O, the reduction potential is shifted negatively.

Nevertheless, both interpretations for the origin of the −0.2 V wave agree with the cathodic ionization mechanism in which oxygen removal can be achieved without the deposition of calcium metal.

3.5. *Microscopic inspection and EDX analysis*

Optical microscopy is very useful to identify oxygen in copper samples because of the formation of the Cu_2O inclusions in the metal phase. This has been demonstrated in Figure 3. For all the samples electrolysed in either of the two molten salts, the image was always free of the Cu_2O inclusions, indicative of an oxygen level lower than 200 ppm [11]. More detailed microscopic work was carried out on a scanning electron microscope. Again, few oxide inclusions were observed. In fact, this is in good agreement with the elemental analysis of some samples as presented in the following Section.

It is known that calcium is completely miscible in molten copper and the two form intermetallic compounds in the solid state [17]. Barium has a very similar property. Therefore, if calcium or barium deposition had occurred during our electrolysis, the corresponding intermetallic compound phases should have been present in the electrolysed samples. On the contrary, both SEM inspections using both secondary and backscattered electrons, and EDX analysis failed to detect any presence of calcium and barium in the electrolysed samples, which is strong evidence for the impurity ionization mechanism proposed in the beginning of this paper.

3.6. *Elemental analysis*

The most convincing evidence of impurity removal came from the fusion elemental analysis of the samples before and after the electrolysis (Table 2). It is worth pointing out that the oxygen levels determined in the two samples electrolysed at 2.1 V are very satisfactory given the short time of electrolysis applied. Taking into account the *IR* drop of the cell and circuit, 2.1 V is much smaller than the theoretical voltages for the decomposition of CaO (2.51 V), BaO (2.14 V), $CaCl_2$ (3.05 V) and $BaCl_2$ (3.30 V) at our working temperature (1160 °C) [5, 6]. This further proves that in our work the molten copper was completely refined in the absence of the deposition of either calcium or barium. Attention is also drawn to that in addition to oxygen, sulfur and selenium have also been removed from the samples to an undetectable level, demonstrating the wide applicability of the cathodic refining technology.

3.7. *Comparison between using graphite and alumina crucibles*

Ward and Hoar raised a question on whether the removal of oxygen could be partly due to the direct reaction between carbon and cuprous oxide [4], for example, $2\,Cu_2O + C = 4\,Cu + CO_2$ (g), $\Delta G°$ (1160 °C) = −269.11 kJ [5, 6]. Our work showed that the oxygen removal was the same whether a graphite or alumina crucible was used, indicative of the important role of electrochemistry.

3.8. *Electrode reactions*

The above results confirm that the ionization of oxygen and other impurities from the molten copper is the main cathodic reaction. At 1160 °C, the solubility of CaO in $CaCl_2$ is about 20 mol% and BaO in $BaCl_2$ about 45 mol% [7, 8], so that the ionized oxygen dissolves in the melt as O^{2-} which is then discharged at the anode. In theory, the discharged oxygen should react with the graphite anode to form carbon mono- or dioxide, which should result in erosion of the graphite anode. However this was not the case as, after the electrolysis, insignificant erosion was observed on the anode, suggesting the formation of oxygen gas. This was confirmed by GC analysis. The chlorine gas did not form in our

experiment as indicated by both the smell and GC analysis of the effluent gases from the electrolysis reactor.

Therefore, the electrode reactions can be expressed as follow:
at cathode:

$$O - Cu = O_{m|e} \quad \text{(diffusion)}$$

(O – Cu represents oxygen dissolved in molten copper)

$$O_{m|e} + 2e^- = O^{2-}$$

at anode:

$$O^{2-} = \tfrac{1}{2}O_2 + 2e^- \quad \text{(main reaction)}$$
$$O^{2-} + C = CO + 2e^- \quad \text{(side reaction)}$$
$$2O^{2-} + C = CO_2 + 4e^- \quad \text{(side reaction)}$$

These reactions are different from those proposed by Ward and Hoar [4] where the evolution of chlorine was considered to be the main anodic reaction with the oxygen remaining as barium oxide in the barium chloride melt.

3.9. *Recessed channel cell*

The results and discussion given in previous sections demonstrate that the electrolytic method is an effective way for the removal of nonmetallic impurities from copper. However, should the static electrolysis be scaled up in industry, the time taken for the electrolysis would be dependent on the depth of the molten copper pool because of the diffusion of impurities to the metal|electrolyte interface. Even though increased convection by, for example, mechanical stirring would help to speed up the reaction, the batch nature of electrolysing a static pool is still a negative factor for an economical consideration. Ward and Hoar [4] highlighted this problem by pointing out that to treat 120 tons per day of blister copper would have required 60 m^2 of horizontal copper pools.

These problems may be solved by the use of the recessed channel electrode (RCE) [9, 10] in which the molten metal flows down channels in the electrode surface creating a well mixed phase with small diffusion distances. Experiments based on this novel RCE were carried out successfully (details Section 2). Figure 7 displays a photograph of a modified RCE cathode used in this work for the electrolysis of oxygenated copper samples. After electrolysis, most of the solidified copper was found near the exit of the RCE, but some blobs and beads remained in the semispherical portions of the channels. This is strong evidence that the molten copper exuded out of the reservoir had gone through the recessed channels. The resulting samples were inspected under an optical microscope and, as expected, no Cu_2O phase was observed.

We would like to highlight the prospects of the industrial application of this novel RCE. Assuming a current density of 0.2 A cm^{-2} and that each recessed electrode has a surface area of 1 m^2, this would remove

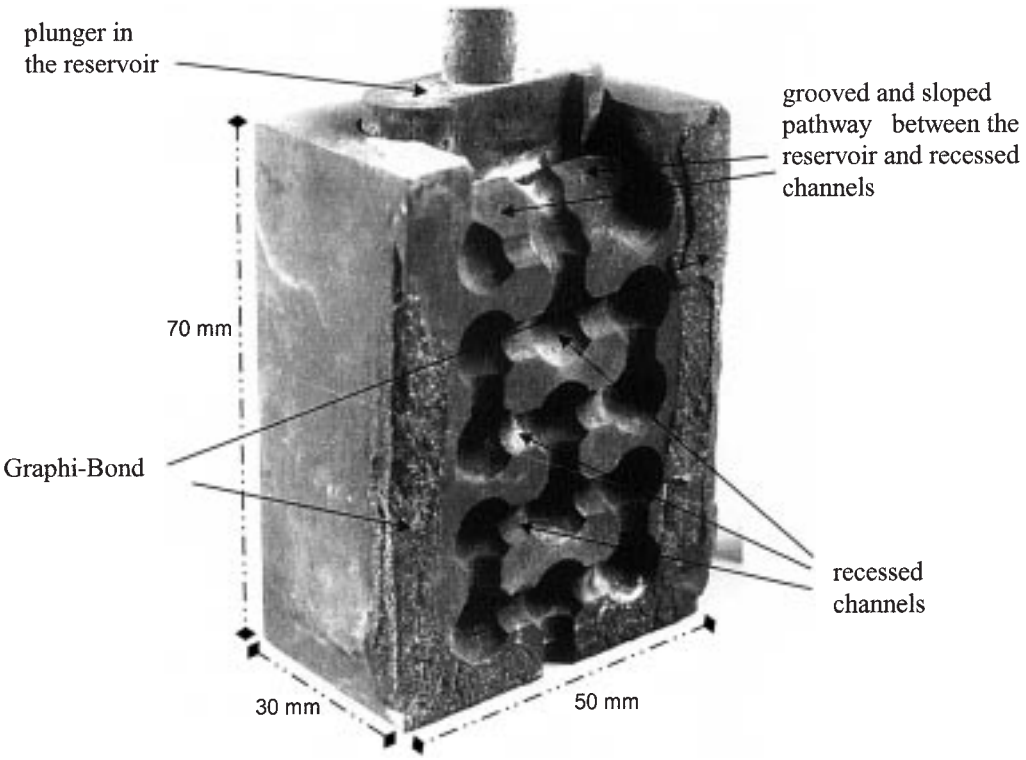

Fig. 7. Photograph of recessed channel electrode used in this work.

1.2 kg of oxygen per electrode per hour. For 120 tons per day containing 0.1% oxygen, this corresponds to four electrodes so that a 200 000 ton per year production of blister copper could be treated by 20 electrode pairs which would occupy a space of roughly 1.5 m × 1.5 m × 3 m, which is significantly less than the 60 m^2 quoted by Ward and Hoar. The electrical costs for the removal of all this oxygen is around £50 assuming 100% current efficiency and 5 p per kWh for electricity.

4. Conclusions

(i) Oxygen, sulfur and selenium contained in molten copper (cathode) can be removed electrochemically in either molten $BaCl_2$ or $CaCl_2$ or the eutectic mixture of the two.

(ii) $BaCl_2$ is a better melt for the electrolysis in comparison with $CaCl_2$ in terms of residual current and also the purity of the refined copper. However, because $CaCl_2$ is much cheaper than $BaCl_2$, it may also be a good candidate for industrial applications.

(iii) The relatively low voltages used in this work, SEM inspections and EDX analysis of the electrolysed samples, and the preliminary voltammetric result suggest the refining mechanism to be the cathodic ionization of the impurities, particularly oxygen. The ionized impurities dissolves in the melt and is then, at least for oxygen, discharged at the anode. The anodic product was a mixture of oxygen and carbon oxides. Chlorine was not detected during the electrolysis.

(iv) A thermodynamic estimation suggested that there may be direct interactions between oxygenated copper and the molten salts used, particularly $CaCl_2$, leading to the dissolution of Cu_2O into the molten salt. If so, our work shows that most of the lost metal can be recovered at relatively high voltages and/or longer times of electrolysis.

(v) Refining molten copper in a recessed electrode cell has been demonstrated and simple calculations showed that this approach can offer a greater space–time-yield than the simple pool cell. Furthermore, the energy costs for the cathodic refining are shown to be virtually negligible.

Acknowledgements

The authors are grateful for samples and chemical analysis from IMI Refiners Ltd, discussions with Drs T. W. Farthing and F. Tailoka, and the financial support from EPSRC. Dr Tailoka also helped on analysing the effluent gases by GC.

References

1. B. Deo and R. Boom, 'Fundamentals of Steelmaking Metallurgy' (Prentice Hall, New York, 1993), p. 300.
2. A.K. Biswas and W.G. Davenport, 'Extractive Metallurgy of Copper' (Pergamon Press, Oxford, 1976), p. 438.
3. K. Grojtheim, C. Krohn, M. Malinovsky and J. Thonstad, 'Aluminium Electrolysis' (Aluminium-Verlag, Dusseldorf, 1997), p. 350.
4. R.G. Ward and T.P. Hoar, *J. Inst. Met.* **90** (1961) 6–12.
5. 'HSC Chemistry for Windows, Outokumpu Research, Finland (1994).
6. D.R. Lide (Ed) 'CRC Handbook of Chemistry and Physics', 77th edn (CRC Press, Boca Raton, FL, 1996).
7. E.M. Levin and H.F. McMurdie, 'Phase Diagrams for Ceramists', 1975 Supplement (American Ceramic Society, Columbus, OH, 1975), p. 394.
8. E.M. Levin, C.R. Robbins and H.F. McMurdie, 'Phase Diagrams for Ceramists' (American Ceramic Society, Columbus, OH, 1964), p. 394.
9. K.J. Driscoll and D.J. Fray, *Trans. IMM.* **102** (1993) C109–117.
10. F. Tailoka and D.J. Fray, *Trans. IMM.* **104** (1995) C51–8.
11. 'Metals Handbook', Vol. 7, 'Atlas of Microstructures of Industrial Alloys', 8th edn (American Society for Metals, OH 1972), p. 273.
12. D.W. McKee, *Carbon* **20** (1982) 59–66.
13. D.W. McKee, C.L. Spiro and E.J. Lamby, *Carbon* **22** (1984) 285–290.
14. O. Yamamoto, T. Sasamoto and M. Inagaki, *Carbon* **33** (1995) 359–365.
15. W. Cermignani, T.E. Paulson, C. Onneby and C.G. Pantano, *Carbon* **33** (1995) 367–374.
16. U. Stohr and W. Freyland, *Phys. Chem. Chem. Phys.* **1** (1999) 4383–4387.
17. H. Massalski (Ed) 'Binary Alloy Phase Diagrams' (ASM International, The Materials Information Society, US, 1990), Ca–Cu, Vol. 1, p. 907, Cu–Ba, Vol. 1, p. 573 and O–Cu, Vol. 2, p. 1447.